Ferroelectricity in Barium Titanate Quantum Dots and Wires

Huaxiang Fu and L. Bellaiche
Department of Physics, University of Arkansas, Fayetteville, Arkansas 72701, USA

(Received 1 August 2003; published 18 December 2003)

Properties of $BaTiO_3$ colloidal quantum dots and wires are simulated using a first-principles-based approach. Large atomic off-center displacements (that are robust against capping matrix materials) are found to exist in very small (<5 nm) dots. We further determine the size dependences of electrical and electromechanical responses in the studied nanostructures, as well as provide microscopic understanding of these responses.

DOI: 10.1103/PhysRevLett.91.257601 PACS numbers: 77.80.–e, 77.65.–j, 61.46.+w

Intense experimental effort has been made recently in synthesizing and understanding ferroelectric (FE) nanostructures—e.g., $BaTiO_3$ dots [1], rods [2], wires [3], and nanotubes [4], and $Pb(Zr, Ti)O_3$ thin films [5,6] and nanoparticles [7]—mainly because of their promise in increasing FE nonvolatile-memory density thousands fold by reading and writing into *individual nanoparticles* [3,8,9]. Furthermore, these FE nanostructures are also critical in light of miniaturizing piezoelectric transducers and actuators, ultrasonic devices, and medical imaging detectors [10,11]. From a fundamental point of view, ferroelectricity is caused by atomic off-center displacements, resulting from a delicate balance between long-range (LR) Coulomb interaction and short-range (SR) covalent interaction [12]. In nanostructures, both interactions—and thus their balance—are altered with respect to the bulk, since the LR interaction is truncated due to lack of periodicity, while the SR one is significantly modified near the surface boundary. Consequently, it is commonly believed [13–16] that ferroelectricity in nanostructures would disappear entirely (i.e., there is no ferroelectric off-center instability) below a critical size. This belief has recently received support from a theoretical study on $BaTiO_3$ *thin films* [17]. For FE nanoparticles, while measurements of lattice structures (rather than polarization) are available only at large sizes (~500 Å, Refs. [14,15]), the critical size of ferroelectricity (if any) is unknown [1–3,7]. In fact, it is not even clear whether there are any ferroelectric displacements in FE dots and/or whether these displacements are aligned to form long-range ferroelectric phases. Similarly, virtually nothing is known about the electrical and mechanical responses of FE nanoparticles to electric fields.

The purpose of this Letter is to investigate, from first principles, the ferroelectric properties of $BaTiO_3$ colloidal nanoparticles—and, in particular, to answer whether there is ferroelectricity in FE nanoparticles *and* how these particles respond to applied electric fields. These properties are found to be unusual and differ from what is commonly believed.

Here, we further develop and use a first-principles-derived effective-Hamiltonian approach [18,19] coupled with Monte Carlo simulations. (Ideally, one would like to use direct first-principles density-functional theory, but this is currently computationally impracticable.) The effective Hamiltonians of Refs. [18,19], which are derived from first principles and possess a comparable accuracy, have been successfully applied to many FE materials, including simple $BaTiO_3$ [20], $PbTiO_3$ [21], and $KNbO_3$ [22] systems, and complex $Pb(Zr, Ti)O_3$ [19] and $Pb(Sc, Nb)O_3$ [23] solid solutions. In this approach, local modes $\{\mathbf{u}_i\}$ (i is the cell index) describe the ferroelectric instability in individual 5-atom cells; $\mathbf{u}_i$ are associated with local electrical dipoles $\mathbf{P}_i$ via $\mathbf{P}_i = Z^* \mathbf{u}_i$ (where Z^* is the effective charge of the local mode).

Compared to the original method detailed in Ref. [18], two new developments are made here in order to be able to study FE nanoparticles: (i) No supercell periodic boundary conditions are imposed, and the LR dipole-dipole interaction is performed in real-space (inside the nanoparticles) rather than in reciprocal space. Our simulations with open-boundary condition precisely mimic the experimental situations [3,5,6] in which polarizations in FE wires and films are probed by noncontact electrostatic forces without metallic electrodes. By contrast, the calculations of $BaTiO_3$ *thin films* in Ref. [17] assume a short-circuit boundary condition with metallic electrodes surrounding the films. Also note that, in our real-space implementation without artificial periodicity for finite systems, the potential field generated by *every* dipole in the nanoparticles—including the depolarization field produced by the charges (i.e., uncompensated dipoles) at nanoparticle surfaces—is precisely computed and properly accounted for. (ii) Existence of the vacuum surrounding nanoparticles will cause *surface-induced* atomic relaxations and cell-shape changes (thus affecting both local modes and local inhomogeneous strains) near the nanoparticle surfaces. To account for the effect of atomic relaxations on local modes, an interaction between local modes at surfaces and the vacuum (denoted as mode-vacuum interaction) is added in the

Hamiltonian. Similarly, an interaction between the inhomogeneous strains and the vacuum (denoted as local strain-vacuum interaction) is added to account for the effect of cell-shape changes on local strains. The parameters of these two SR interactions—whose contributions to total energy are analytically similar to the species-dependent intersite coupling terms of Ref. [19]—are determined from first-principles local-density-approximation (LDA) calculations on $BaTiO_3$ surfaces. Our effective Hamiltonian for FE dots thus includes the dominating effects caused by the vacuum on charge redistribution, atomic relaxations, and cell-shape changes near the surfaces. We assume that the surfaces of nanoparticles are BaO terminated, since they have lower energies than TiO-terminated surfaces [24]. Other interaction parameters used here (to describe the FE material *per se*) are those of Ref. [20] for *bulk* $BaTiO_3$, since Ref. [17] demonstrates that these parameters do not change significantly when going from bulk to nanostructures. Local modes $\{\mathbf{u}_i\}$ at low temperatures are obtained via temperature-annealing Monte Carlo simulations. A pressure of -4.8 GPa is used in simulations to correct the LDA error in lattice constant. Results presented here are obtained for 50 K.

For simplicity, we assume $BaTiO_3$ dots to be rectangular, since adopting a spherical or a square cross section leads only to a minor difference. The rectangular dots are denoted as $n_x \times n_y \times n_z$, where n_x, n_y, n_z are the numbers of five-atom cells contained in the dots along the pseudocubic [100], [010], and [001] directions, respectively. The average size of a nanoparticle is thus given by $L = (L_x L_y L_z)^{1/3}$, where $L_i = n_i a$ $(i = x, y, z)$ are the lengths along the three Cartesian axes ($a = 4.0$ Å is the lattice constant of $BaTiO_3$). For the clarity of demonstration, our prediction for local modes $\{\mathbf{u}_i\}$ will be presented on a certain perovskite *B*-site plane, which is specified by its normal direction and its order index among the equivalent planes (e.g., the $y = 6$ plane is the 6th plane having a normal direction along the y axis).

Local modes $\{\mathbf{u}_i\}$ on the $y = 6$ plane of a $12 \times 12 \times 12$ dot are depicted in Fig. 1(a). Significant ferroelectric off-center displacements can be clearly seen in this small ($L = 4.8$ nm) dot. The local-mode *magnitude* $\langle|\mathbf{u}|\rangle$, averaged over all 5-atom cells, is $0.043a$ in this dot. This is remarkably large and comparable with the value of $0.039a$ found in bulk $BaTiO_3$. These large off-center displacements, indicating the existence of significant dipoles in each cell, have an important implication—that is, a *large* amount of macroscopic polarization can be generated by aligning these local dipoles with electric fields. Note that this effect cannot be achieved in nonferroelectric nanoparticles *without* off-center displacements, unless a huge electric field is applied. In fact, other calculations we performed (not shown here) predict that large off-center displacements yielding a magnitude $\langle|\mathbf{u}|\rangle = 0.052a$ occur even in the tiny $4 \times 4 \times 4$ dot ($L = 1.6$ nm). Conceivably, such a small size is likely the limit achievable in experiments. These results thus suggest that there is virtually no critical size for ferroelectric instability in nanoparticles.

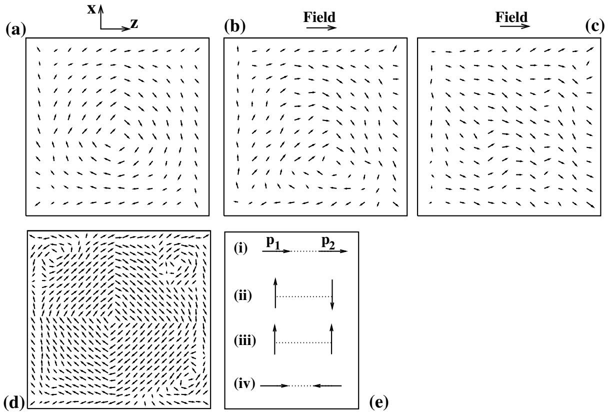

FIG. 1. (a) Local-mode displacements, $\{\mathbf{u}_i\}$, of the cells centered on the $y =$ 6th *B* plane of the $12 \times 12 \times 12$ dot under zero electric field. The arrows give the direction of these displacements, projected on the xz plane, and the arrow length indicates the *projected* magnitude. (b) The same as (a), but under a field of $E = 5 \times 10^8$ V/m applied along the z axis. (c) The same as (a), but under a field of $E = 10^9$ V/m applied along the z axis. (d) Local-mode displacements $\{\mathbf{u}_i\}$ of the cells centered on the $y =$ 12th *B* plane of the $24 \times 24 \times 24$ dot. (e) Illustrations of four specific configurations of two dipoles with fixed centers but different orientations. Note that the dipole-dipole electrostatic energy increases from (i) to (iv). The dipoles axis (dotted line) is defined as the straight line connecting the centers of two dipoles. (For enlarged figure, see [25].)

For the dipoles on the dot surfaces, analysis of Fig. 1(a) shows that the *parallel-to-surface* components of these dipoles prefer to point along opposite directions on two opposite surfaces, while the (small) *normal-to-surface* components tend to bulge out due to the surface-induced atomic relaxations. Figure 1(a) further reveals that the local dipoles in small dots prefer to rotate from cell to cell, forming an unusual and complex "vortex-like" pattern (similar to the ones found in some magnetic compounds). Note that this vortex pattern in FE dots is different from the ferroelectric pattern in bulk (where all dipoles are aligned along the same direction, as predicted by similar-size supercell effective-Hamiltonian simulations or assumed in five-atom first-principles calculations). Interestingly, as a result of the dipole pattern in Fig. 1(a) the total *macroscopic* polarization is found to be zero (i.e., $\langle\mathbf{u}\rangle = 0$). Furthermore, we found that the vortex pattern of displacements does *not* alter appreciably when turning off and on the mode-vacuum SR interaction. This suggests another important conclusion, namely, that ferroelectric instability in dots is not much affected by the surface local environments or, equivalently, that *the capping organic matrix materials used in experiments should not affect the ferroelectric properties of the dots.* Unlike in Ref. [17] where charges in *metallic* electrodes are able to move freely and will thus cause strong screening, the organic capping materials used in colloidal FE nanoparticles [1,2,7] are insulators of large gap (~10 eV) and the resulting screening is very small. As the dot increases in size to 24 × 24 × 24, the local FE displacements tend to order between each other via the formation of eight rather uniform ferroelectric domains [Fig. 1(d)]. The polarization of each domain in Fig. 1(d) is found to point along one of the eight pseudocubic [± 1 ± 1 ± 1] directions. The macroscopic polarization of the entire dot remains as zero.

The displacement pattern in Fig. 1(a) results from a new balance (with respect to the bulk case) between the LR and SR interactions in dots, and can be simply explained as follows. First, let us consider the LR dipole-dipole interaction alone for two isolated dipoles [with four specific orientations illustrated in Fig. 1(e)]; the lowest-energy configuration is that these two dipoles both point at the same direction along the dipole axis [case (*i*) in Fig. 1(e)]. Indeed, it can be seen in Fig. 1(a) that the dipoles belonging to a same row have their parallel-to-dipole-axis (i.e., the z axis) components aligned along the same direction. (Note that dipoles on the dot surfaces are exceptions, see below.) Next, let us select a given row in Fig. 1(a), and note that the dipoles located near the nanoparticle surfaces in this row tend to have large parallel-to-surface ("in-plane") components with their normal components suppressed by the vacuum; these inplane components (being perpendicular to the dipole axis) shall flip their directions [since case (*ii*) has a lower energy than case (*iii*) in Fig. 1(e)]. However, this flip of the component perpendicular to the z axis does not occur within the nearest cell [see Fig. 1(a)], since we found that it will otherwise drastically increase the short-range energy. Instead, the flip occurs *across the entire dot*, forming the unusual pattern in Fig. 1(a).

Now we turn our attention to electric-field effects in nanoparticles. More precisely, we are particularly interested in revealing the size dependences of these effects. We decide to elongate the nanoparticles only along the z axis (that is, the applied-field direction) to mimic quantum wires, partly because increasing the dot size along all three dimensions is computationally prohibitive. Figure 2(a) shows the resulting *net* z axis mode average $\langle \mathbf{u}_z \rangle$ and clearly indicates that the same electric field induces a larger polarization *per five-atom cell* in a long wire than in a short wire. Field effects in FE dots thus depend substantially on sizes. This is the first time that the size dependence of field-induced polarization is firmly established (to our knowledge). Figure 2(a) further reveals that a *small* electric field in long wires drives a *rapidly* increasing polarization and thus *easily* turns a (macroscopically) paraelectric FE nanostructure into a (macroscopically) ferroelectric phase. Here we define the poling field E_{pf} as the field that is needed to drive a net average displacement $\langle \mathbf{u}_z \rangle$ equal to the bulk value of 0.02a. The poling fields for different-size wires are given in Fig. 2(b), and drastically *decrease* when increasing size. More precisely, fitting our theoretical data in Fig. 2(b) as a function of size gives $E_{pf} = 38.1966/L_z^n$ with $n = 0.7821$, where E_{pf} is in unit of 10^8 V/m and L_z in unit of nm.

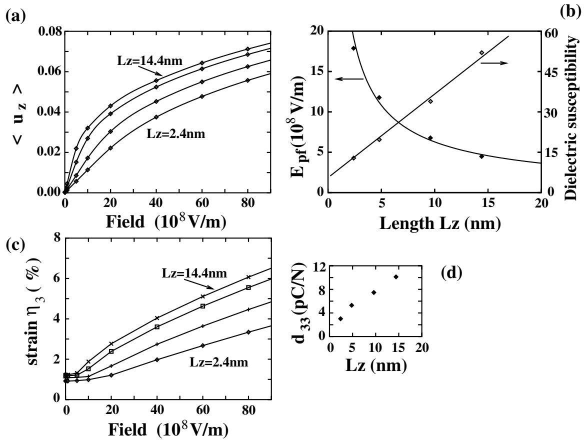

FIG. 2. (a) Response of the net mode-average $\langle \mathbf{u}_z \rangle$ per unit cell, in unit of bulk lattice constant, as a function of electric field in quantum wires of different lengths. Four curves, from bottom to top, correspond to $L_z = 2.4$, 4.8, 9.6, and 14.4 nm, respectively. The x-axis and y-axis lengths are both fixed at 4.8 nm. (b) Dependences of the poling field (E_{pf}) and the dielectric susceptibility (of stage I) on the wire length L_z. This susceptibility is different from the calculated bulk value of ~124, since the latter does not correspond to dipole flipping. (c) Response of the strain η_3 to the applied electric fields in four different wires considered in (a). (d) Piezoelectric coefficient d_{33} (of stage II) as a function of the wire length. Symbols in this figure show the direct results of the simulations, while lines are guides for eyes [except in (b), where the analytically fitted result for the poling field is shown].

Our predictions provide explanations and/or suggest reinterpretations of many experimental results. For instance, no detectable polarizations were probed by electrostatic force microscopy along the perpendicular directions of both *as-deposited* $BaTiO_3$ nanowires [3] and *as-grown* PZT films [5]. This can be simply explained by the vanishing net polarizations we found in dots and in wires [see, e.g., Fig. 1(a)]. Our findings further suggest that the nondetectable polarization in PZT films may not be due to the electrostatic passivation of additional charges at sample surfaces as it was speculated [5], but rather results from the "intrinsic" arrangement of local dipoles. Moreover, it was found experimentally [3] that a field of 3.6×10^8 V/m is needed to "write" a polarization along the perpendicular direction of an 18 nm-diameter $BaTiO_3$ wire, which is in excellent agreement with our predicted value of 3.98×10^8 V/m obtained from the formula given above.

We now provide a microscopic understanding of the field-induced responses in FE dots. We find that the responses in Fig. 2(a) can be separated into three stages according to their $\langle u_z \rangle$-vs-field behaviors, and here we use the $12 \times 12 \times 12$ dot to illustrate these stages. (1) At stage I (that occurs at field $E < 10^9$ V/m), the dipoles pointing opposite to the field direction are sequentially *flipped* [Fig. 1(b)]. The flip process occurs first near the domain boundary, while dipoles on the dot surface are found to be more resistant to the applied field [see Fig. 1(b)]. Stage I generates a polarization that varies *linearly* with the field strength [Fig. 2(a)]. The slope (i.e., dielectric susceptibility) is given in Fig. 2(b) for different wires and is found to increase linearly with the wire length. (2) At stage II ($10^9 < E < 4 \times 10^9$ V/m), the dipoles start to *rotate* towards the field direction as the dipole flips of stage I have been completed [Fig. 1(c)]. Stage II differs from the polarization rotation in bulk [26,27] in that, prior to the rotation, local dipoles in dots are not parallely aligned as in bulk. Interestingly, this second stage yields a strong *nonlinear* field dependence of polarization [Fig. 2(a)]. (3) At stage III ($E > 4 \times 10^9$ V/m), with the dipoles having all been previously rotated along the field direction, the magnitude of each dipole then starts to be *enlarged* by the field, resulting in a nearly linear field-dependent polarization again.

Finally, we examine the electromechanical response in FE wires. The field-induced η_3 strains are depicted in Fig. 2(c). At stage I, the strain response is found to be surprisingly small though there is a rapid increase in polarization, which suggests that polarization *does not* couple with strain during the dipole flipping process. At stage II, the strain increases evidently with the field strength [Fig. 2(c)]; the strain-vs-field slope is the piezoelectric coefficient d_{33}. The d_{33} values are given in Fig. 2(d) for different wires, and exhibit a *monotonous increase* with size. Interestingly, the d_{33} coefficients in nanoparticles ($\sim$10 pC/N) are found to be much smaller than in bulk ($\sim$77 pC/N), suggesting that the electromechanical response can be *drastically modified* by varying sizes.

In summary, we have performed a pioneering study of ferroelectric quantum dots and wires using a microscopic first-principles based approach. We find: (i) Large ferroelectric off-center displacements exist in very small ($\sim$5 nm) dots. This result solves a long-standing puzzling question in experiments, namely, whether there exists ferroelectricity in colloidal FE dots *under zero field.* This discovery also opens a possibility of tremendous increase in FE-memory density. (ii) FE displacements in dots exhibit an unusual and hitherto-unknown vortex pattern. This pattern is found to cause rather peculiar field-induced polarization responses. (iii) The ferroelectric instability in dots is found to be robust against the organic capping materials. (iv) The poling field is predicted to decrease drastically with increasing size, which is important for practical controls of FE nanostructures by use of external electric fields. (v) The polarization responses of FE dots at stage II are found to be strongly nonlinear, while the electromechanical responses in dots are found to be remarkably smaller than those in the bulk.

We thank J. Iniguez and D. Vanderbilt for sharing their parameters of bulk $BaTiO_3$, and A. Garcia, Ph. Ghosez, and I. Kornev for helpful discussions. This work was supported by the Office of Naval Research (N00014-01-1-0366, N00014-03-1-0598, N00014-01-1-0600), Center for Piezoelectrics by Design, National Science Foundation (DMR-0116315, DMR-9983678), and Arkansas-Oklahoma MRSEC.

[1] S. O'Brien, L. Brus, and C. B. Murray, J. Am. Chem. Soc. **123**, 12 085 (2001).
[2] J. J. Urban, W. S. Yun, Q. Gu, and H. Park, J. Am. Chem. Soc. **124**, 1186 (2002).
[3] W. S. Yun *et al.*, Nano Lett. **2**, 447 (2002).
[4] Y. Luo *et al.*, Appl. Phys. Lett. **83**, 440 (2003).
[5] C. H. Ahn *et al.*, Science **276**, 1100 (1997).
[6] T. Tybell, C. H. Ahn, and J.-M. Triscone, Appl. Phys. Lett. **75**, 856 (1999).
[7] C. Liu *et al.*, J. Am. Chem. Soc. **123**, 4344 (2001).
[8] J. F. Scott and C. A. Paz de Araujo, Science **246**, 1400 (1989).
[9] O. Auciello, J. F. Scott, and R. Ramesh, Phys. Today **51**, No. 7, 22 (1998).
[10] M. E. Lines and A. M. Glass, *Principles and Applications of Ferroelectrics and Related Materials* (Clarendon, Oxford, 1979).
[11] K. Uchino, *Piezoelectric Actuators and Ultrasonic Motors* (Kluwer Academic, Boston, 1996).
[12] R. E. Cohen, Nature (London) **358**, 136 (1992).
[13] S. Li *et al.*, Jpn. J. Appl. Phys., Pt. 1, **36**, 5169 (1997).
[14] S. Chattopadhyay *et al.*, Phys. Rev. B **52**, 13 177 (1995).
[15] K. Ishikawa *et al.*, Jpn. J. Appl. Phys., Pt. 1, **35**, 5196 (1996).
[16] T. Maruyama *et al.*, Appl. Phys. Lett. **73**, 3524 (1998).
[17] J. Junquera and Ph. Ghosez, Nature (London) **422**, 506 (2003).
[18] W. Zhong, D. Vanderbilt, and K. M. Rabe, Phys. Rev. Lett. **73**, 1861 (1994).
[19] L. Bellaiche, A. Garcia, and D. Vanderbilt, Phys. Rev. Lett. **84**, 5427 (2000).
[20] J. Iniguez and D. Vanderbilt, Phys. Rev. Lett. **89**, 115503 (2002).
[21] Ph. Ghosez and K. M. Rabe, Appl. Phys. Lett. **76**, 2767 (2000).
[22] H. Krakauer, R. Yu, C. Z. Wang, and C. Lasota, Ferroelectrics **206**, 133 (1998).
[23] A. M. George, J. Iniguez, and L. Bellaiche, Nature (London) **413**, 54 (2001).
[24] J. Padilla and D. Vanderbilt, Phys. Rev. B **56**, 1625 (1997).
[25] See http://comp.uark.edu/~hfu/download.html for enlarged Fig. 1.
[26] H. Fu and R. E. Cohen, Nature (London) **403**, 281 (2000).
[27] A. Garcia and D. Vanderbilt, Appl. Phys. Lett. **72**, 2981 (1998).